



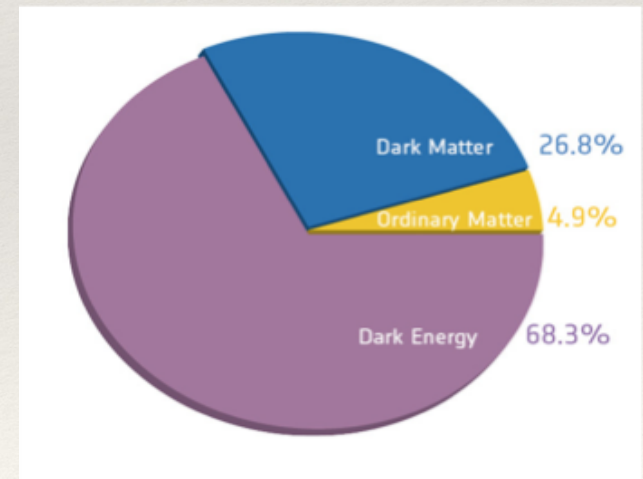
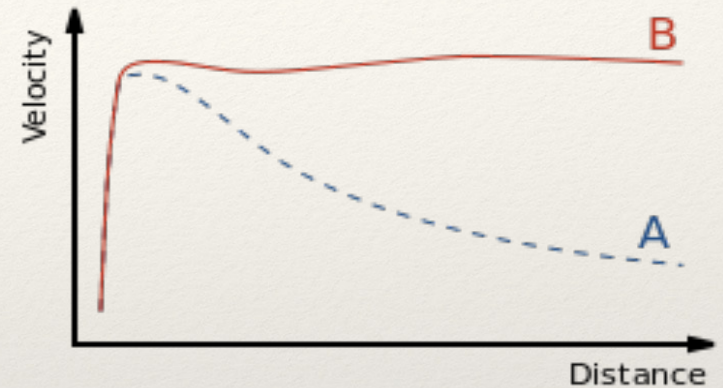
ICHEP2018 SEOUL

A frequentist analysis of proton-philic spin-dependent inelastic Dark Matter (pSIDM) as an explanation of the DAMA effect

Jong-Hyun Yoon @ Sogang U.
In collaboration with
Prof. Stefano Scopel
Dr. Gaurav Tomar
Mr. Sunghyun Kang

Introduction

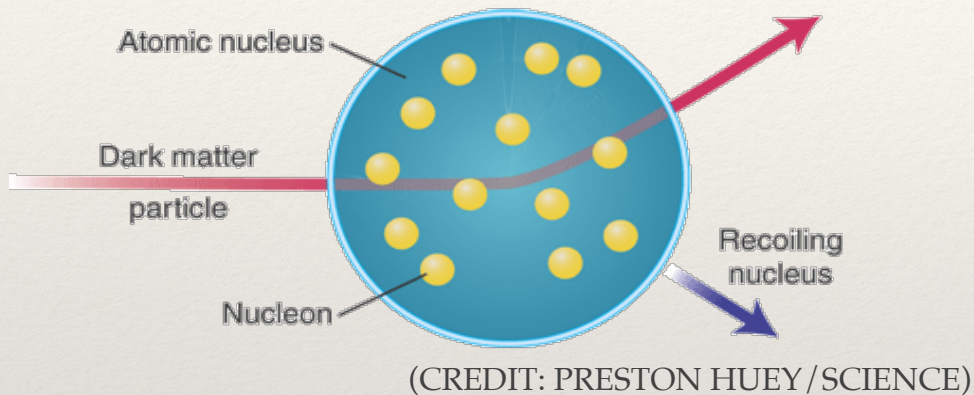
- ❖ Dark Matter and the Standard Model
- ❖ Numerous evidences
- ❖ A variety of candidates
- ❖ WIMP (Weakly Interacting Massive Particle)
- ❖ Worldwide efforts to search for DM



(Credit: ESA and the Planck Collaboration.)

Introduction

❖ Dark Matter Direct Detection



(COSINE-100 Dark Matter Experiment)

❖ WIMP rates

$$R_{[E'_1, E'_2]} = MT \int_{E'_1}^{E'_2} \frac{dR}{dE'} dE'$$

$$\frac{dR}{dE'} = \sum_T \int_0^\infty \frac{dR_{\chi T}}{dE_{ee}} \mathcal{G}_T(E', E_{ee}) \epsilon(E') dE_{ee}$$

$$E_{ee} = q(E_R) E_R,$$

proton–philic Spin–dependent Inelastic Dark Matter (pSIDM)

Germanium experiments carry only a very small amount of ^{73}Ge , the only isotope with spin, **carried by an unpaired neutron**

Isotope	Spin	Z (# of protons)	A-Z (# of neutrons)	Abundance
^{73}Ge	9/2	32	41	7.7 %

Xenon experiment contain two isotopes with spin, **both carried mostly by an unpaired neutron**

Isotope	Spin	Z (# of protons)	A-Z (# of neutrons)	Abundance
^{129}Xe	$\frac{1}{2}$	54	75	26%
^{131}Xe	3/2	54	77	21%

If the WIMP particle couples only to protons ($c^n / c^p \ll 1$) in a spin-dependent way the rate for Germanium and Xenon detectors is strongly suppressed and their bounds can be evaded

proton–philic Spin–dependent Inelastic Dark Matter (pSIDM)

- ❖ Low v_{\min} can explain the DAMA excess and the null signal from other experiments

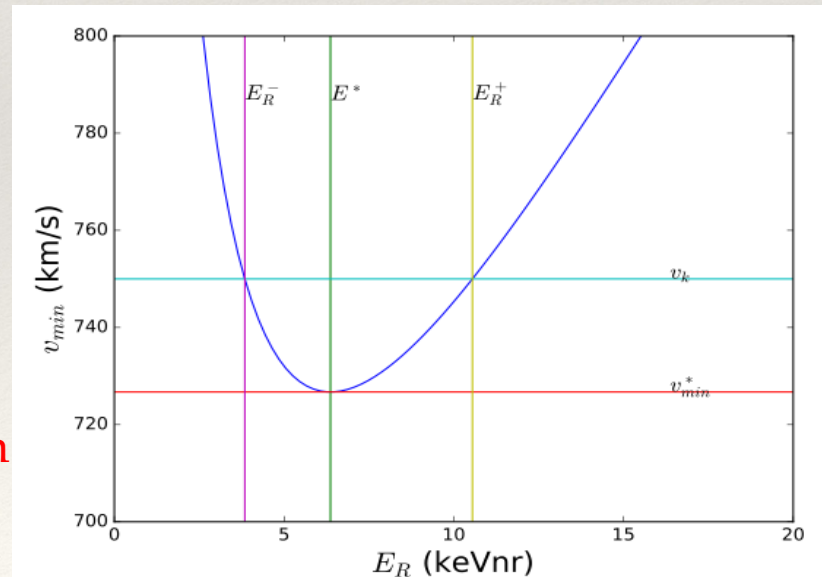
$$\frac{dR_{\chi T}}{dE_R} = N_T \int_{v_{\min}}^{v_{\text{esc}}} \frac{\rho_{\chi}}{m_{\chi}} v \frac{d\sigma_{\chi T}}{dE_R} f(v) dv,$$

$$\int_0^{\infty} dE_R \int_{v_{\min}}^{\infty} dv \rightarrow \int_{v_{\min}^*}^{\infty} dv \int_{E_R^-(v)}^{E_R^+(v)} dE_R, \quad E_R^{\pm}(v_{\min}, m_{\chi}, \delta) = \frac{\mu_{\chi N}^2}{m_N} \left[v_{\min}^2 - \frac{(v_{\min}^*)^2}{2} \pm \sqrt{v_{\min}^2 - (v_{\min}^*)^2} \right],$$

$$v_{\min}^* = \sqrt{\frac{2\delta}{\mu_{\chi N}}}, \quad v_{\min} = \frac{1}{\sqrt{2m_N E_R}} \left| \frac{m_N E_R}{\mu_{\chi N}} + \delta \right|,$$

$$v_{\min}^{*Na} < v_{\text{cut}}^{\text{lab}} < v_{\min}^{*F},$$

For appropriate choice of parameters WIMP-fluorine scatterings can be kinematically forbidden while WIMP-sodium scatterings can explain the DAMA effect



proton–philic Spin–dependent Inelastic Dark Matter (pSIDM)

❖ Non-relativistic effective models

$$\mathcal{H} = \sum_{\tau=0,1} \sum_{k=1}^{15} c_k^{\bar{\tau}} \mathcal{O}_k t^{\tau}, \quad t^0 = 1, t^1 = \tau_3$$

$$\frac{d\sigma_{\chi T}}{dE_R} = \frac{1}{10^6} \frac{2m_T}{4\pi} \frac{c^2}{v^2} \left[\frac{1}{2j_{\chi} + 1} \frac{1}{2j_T + 1} \sum_{spin} |\mathcal{M}_{\mathcal{T}}|^2 \right]$$

$$\frac{1}{2j_{\chi} + 1} \frac{1}{2j_T + 1} \sum_{spin} |\mathcal{M}_{\mathcal{T}}|^2 = \frac{4\pi}{2j_T + 1} \sum_{\tau\tau'} R_l^{\tau\tau'} W_{T,l}^{\tau\tau'}, \quad l=M, \Sigma'', \Sigma', \Phi'', \Phi'' M, \bar{\Phi}', \Delta, \Delta\Sigma'$$

$$R_l^{\tau\tau'} = R_{0,l}^{\tau\tau'} + R_{1,l}^{\tau\tau'} (v^2 - v_{min}^2).$$

$$\mathcal{L}_{int} \ni c^p \vec{S}_{\chi} \cdot \vec{S}_p + c^n \vec{S}_{\chi} \cdot \vec{S}_n,$$

A.L.Fitzpatrick, W.Haxton, E.Katz, N.Lubbers and Y.Xu, JCAP1302, 004

(2013),1203.3542;

N.Anand, A.L.Fitzpatrick and W.C.Haxton, Phys.Rev.C89, 065501

(2014).1308.6288.

proton–philic Spin–dependent Inelastic Dark Matter (pSIDM)

❖ Reassemble the integration

$$R_{[E'_1, E'_2]} = \frac{\rho_\chi}{m_\chi} \sigma_p \int_{v_{min}^*}^{\infty} dv \hat{\mathcal{H}}(v) f(v), \quad \sigma_p = (c_4^p)^2 \frac{\mu_{\chi N}^2}{\pi},$$

$$\begin{aligned} \hat{\mathcal{H}}(v) &= \sum_T N_T M T \frac{c^2 m_T}{v \mu_{\chi T}^2} \frac{2\pi}{10^6} \int_{E_R^-(v)}^{E_R^+(v)} dE_R \int_{E'_1}^{E'_2} dE' \epsilon(E') \mathcal{G}_T[E', q(E_R) E_R] \times \\ &\quad \frac{1}{2j_T + 1} \sum_{\tau\tau'} \sum_l \left[\hat{R}_{0,l}^{\tau\tau'} + \hat{R}_{1,l}^{\tau\tau'} (v^2 - v_{min}^2) \right] W_l^{\tau\tau'} = \\ &\quad \frac{c^2}{v} \int_{E_R^-(v)}^{E_R^+(v)} dE_R \left\{ \hat{\mathcal{R}}_0(E_R) + \hat{\mathcal{R}}_1(E_R) (v^2 - v_{min}(E_R)^2) \right\}, \end{aligned}$$

$$\begin{aligned} \hat{\mathcal{R}}_{\{0,1\}} &= \sum_T N_T M T \frac{m_T}{\mu_{\chi T}^2} \frac{2\pi}{10^6} \int_{E'_1}^{E'_2} dE' \epsilon(E') \mathcal{G}_T[E', q(E_R) E_R] \frac{1}{2j_T + 1} \sum_{\tau\tau'} \sum_l \hat{R}_{\{0,1\},l}^{\tau\tau'} W_l^{\tau\tau'} \\ &= \sum_T \left[\hat{\mathcal{R}}_{\{0,1\}} \right]_T, \quad \hat{R}_{0,l}^{\tau\tau'} \equiv R_{0,l}^{\tau\tau'} / (c_4^p)^2 \end{aligned}$$

proton–philic Spin–dependent Inelastic Dark Matter (pSIDM)

❖ Halo-independent analysis

$$f(v) \equiv -v \frac{d}{dv} \eta(v), \quad R_{[E'_1, E'_2]} = \frac{\rho_\chi \sigma_p}{m_\chi} \int_0^\infty dv \hat{\mathcal{R}}(v) \eta(v) = \int_0^\infty dv \mathcal{R}(v) \tilde{\eta}(v),$$

$$\tilde{\eta}(v, t) = \frac{\rho_\chi \sigma}{m_\chi} \eta(v, t), \quad \eta(v, t) = \int_v^\infty \frac{f(v', t)}{v'} dv', \quad \hat{\mathcal{R}}(v) = \frac{d}{dv} [v \hat{\mathcal{H}}(v)]$$

$$\tilde{\eta}_{0,1}(v) = \sum_{k=1}^N \tilde{\eta}_{0,1}^k \theta(v - v_{k-1}) \theta(v_k - v), \quad \tilde{\eta}_{0,1}^k(v_{min}) = \sum_{i=k}^N \delta \tilde{\eta}_{0,1}^i,$$

$$\begin{aligned} R_{[E'_1, E'_2]} &= N_T M T \frac{\rho_\chi \sigma}{m_\chi} \int_{v_{min}^*}^\infty dv \frac{d}{dv} \left\{ v \frac{c^2}{v} \int_{E_R^-(v)}^{E_R^+(v)} dE_R \left\{ \hat{\mathcal{R}}_0(E_R) + \hat{\mathcal{R}}_1(E_R) [v^2 - v_{min}(E_R)^2] \right\} \right\} \\ &\times \sum_{k=1}^N \delta \tilde{\eta}^k \theta(v_k - v) = N_T M T \frac{\rho_\chi \sigma c^2}{m_\chi} \sum_{k=1}^N \delta \tilde{\eta}^k \times \\ &\int_{E_R^-(v)}^{E_R^{max}(v_k)} dE_R \left\{ \hat{\mathcal{R}}_0(E_R) + \hat{\mathcal{R}}_1(E_R) [v_k^2 - v_{min}(E_R)^2] \right\}. \end{aligned}$$

proton–philic Spin–dependent Inelastic Dark Matter (pSIDM)

❖ DAMA experiment and Annual modulation

Average rate

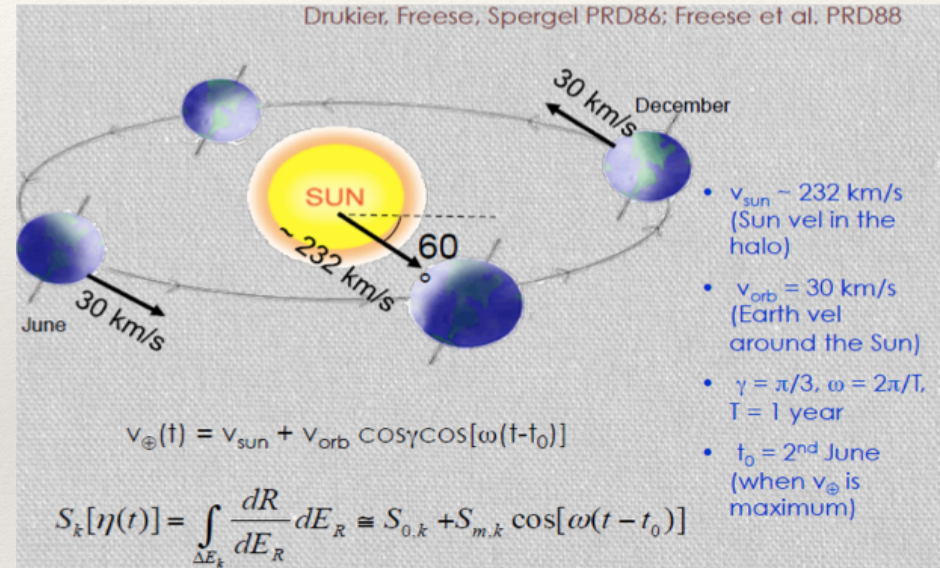
$$S_0 \equiv \frac{1}{T} \int_0^T S(t) dt = \int_0^\infty \mathcal{R}(v) \tilde{\eta}_0(v) dv,$$

$$\tilde{\eta}_0(v) \equiv \frac{1}{T} \int_0^T \tilde{\eta}(v, t) dt,$$

Annual modulation

$$S_1 \equiv \frac{2}{T} \int_0^T \cos \left[\frac{2\pi}{T} (t - t_0) \right] S(t) dt = \int_0^\infty \mathcal{R}(v) \tilde{\eta}_1(v) dv,$$

$$\tilde{\eta}_1(v) \equiv \frac{2}{T} \int_0^T \cos \left[\frac{2\pi}{T} (t - t_0) \right] \tilde{\eta}(v, t) dt,$$



proton–philic Spin–dependent Inelastic Dark Matter (pSIDM)

❖ Likelihood analysis

$$-2 \ln \mathcal{L}(\mathbf{d}|\Theta) = \sum_{n=1}^{N_{DAMA}} \left(\frac{S_{1,n}(\Theta) - S_{1,n}^{exp}}{2\sigma_n^{exp}} \right)^2 - 2 \sum_{i=1}^{N_{exp}} \sum_{j=1}^{N_{bin}^i} \mathcal{L}_j^i(\Theta) \quad \theta \equiv (m_\chi, \delta, r)$$

$$\Theta = (\theta, \eta) \quad -2\mathcal{L}_j^i(\Theta) = 2 \left[S_{0,j}^i(\Theta) + B_j^i - N_j^i - N_j^i \ln \frac{S(\Theta)_{0,j}^i + B_j^i}{N_j^i} \right]$$

$S_{1,n}$ is the prediction of the DAMA modulation amplitude in the n -th bin

$S_{1,n}^{exp}$ the corresponding measurement with error σ_n^{exp}

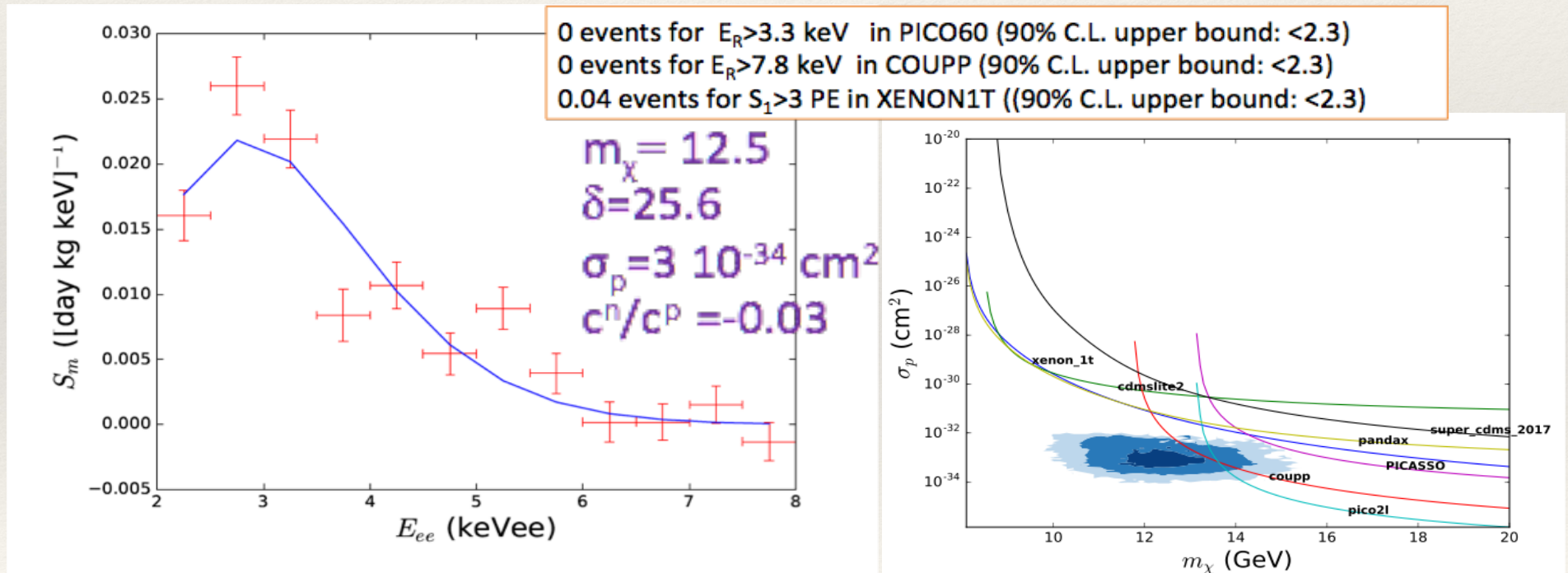
$S_{0,j}^i$ the expected rate in the i -th energy bin of the j -th experiment

N_j^i the corresponding measured count rate

B_j^i the expected background

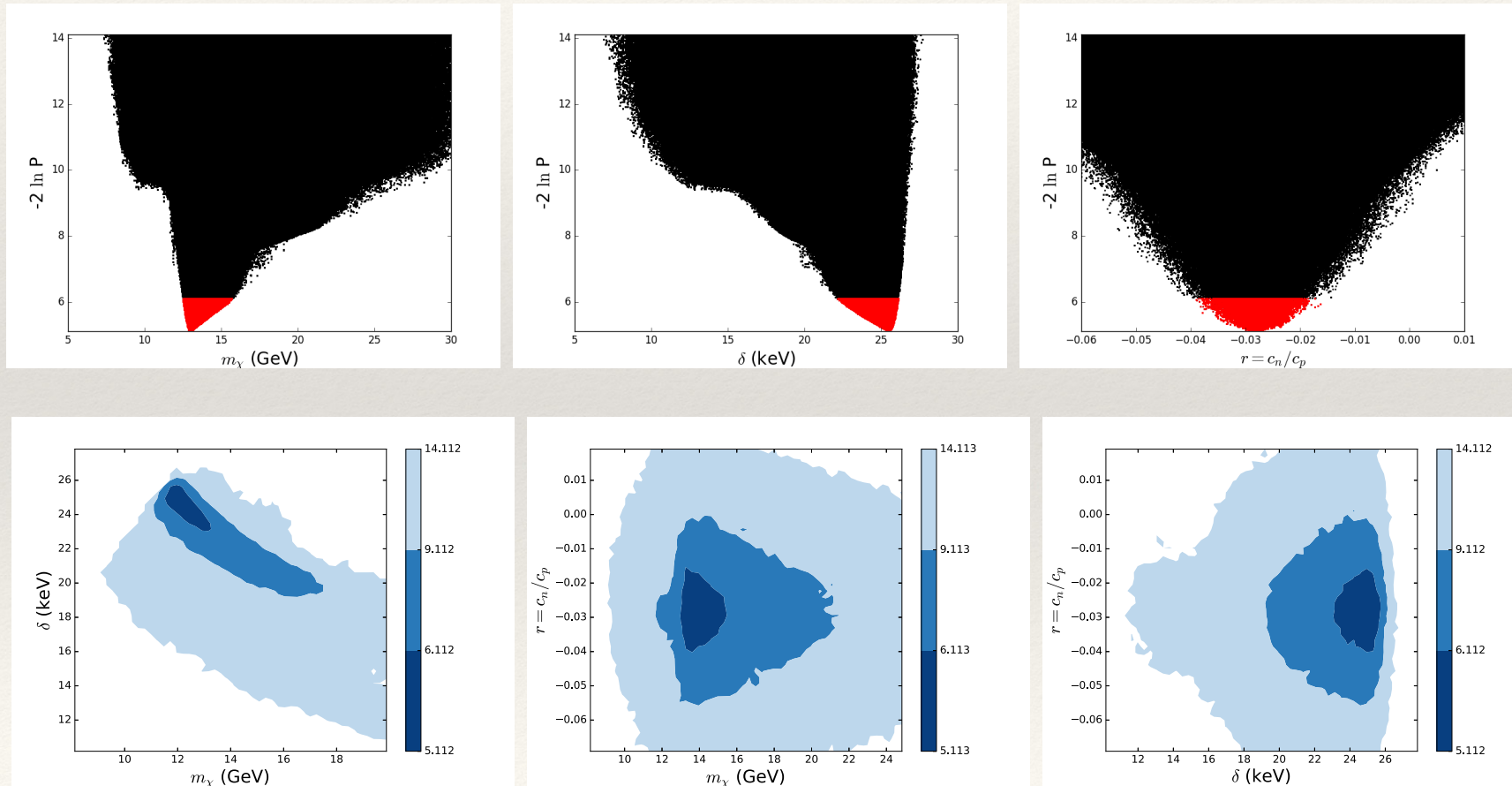
proton-philic Spin-dependent Inelastic Dark Matter (pSIDM)

- ❖ DAMA run 1
- ❖ Best fit: $\chi^2 = 8.5$ with 12-4 d.o.f. (p-value: 0.38)



proton-philic Spin-dependent Inelastic Dark Matter (pSIDM)

DAMA / LIBRA phase-1 (frequentist interval for three parameters: WIMP mass, mass splitting and c^n / c^p)



proton–philic Spin–dependent Inelastic Dark Matter (pSIDM)

DAMA / LIBRA phase-1 (frequentist interval for three parameters: WIMP mass, mass splitting and c^n / c^p)

$$12.5 \text{ GeV} \leq m_\chi \leq 15.7 \text{ GeV}$$

$$22.1 \text{ keV} \leq \delta \leq 26.1 \text{ keV}$$

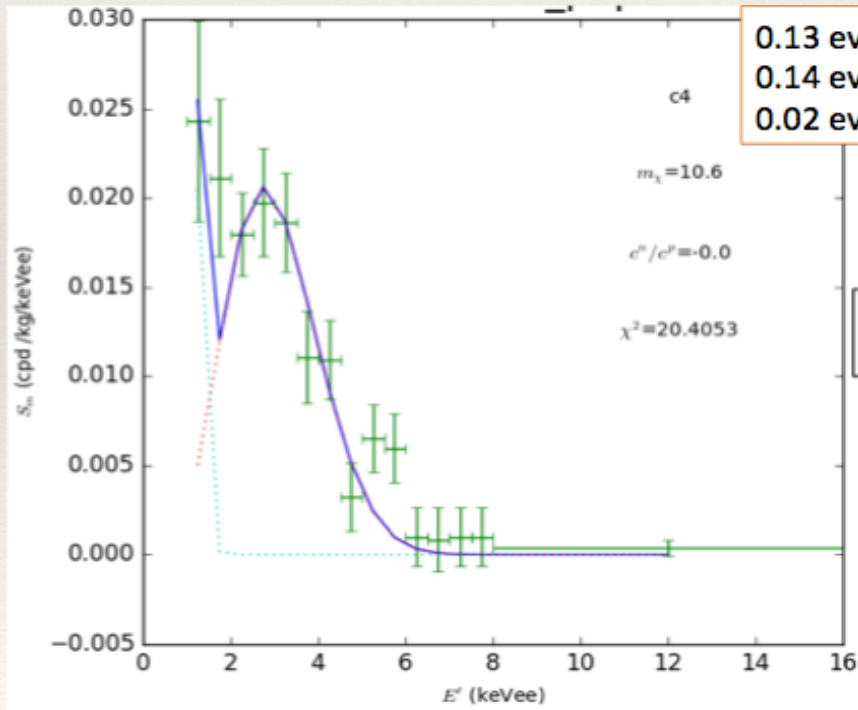
$$-0.039 \leq r \leq -0.016.$$

For this choice of parameters, pSIDM explains DAMA / LIBRA phase-1 in compliance with ALL other constraints!

DAMA/LIBRA phase-2 changed it all : lower threshold brings in WIMP-iodine scatterings

proton-philic Spin-dependent Inelastic Dark Matter (pSIDM)

- ❖ pSIDM update with DAMA run2
- ❖ Harder to fit iodine in the first two bin
- ❖ Best fit: $\chi^2 = 20.4$ with 11 d.o.f. (p-value: 0.04)



$$m_\chi = 10.6$$
$$\delta = 22.5$$
$$\sigma_p = 1.5 \cdot 10^{-33} \text{ cm}^2$$
$$c^n/c^p = 0$$

Work in progress

- We are working on it
- In the meantime today I will discuss DAMA phase2 in non-relativistic effective models





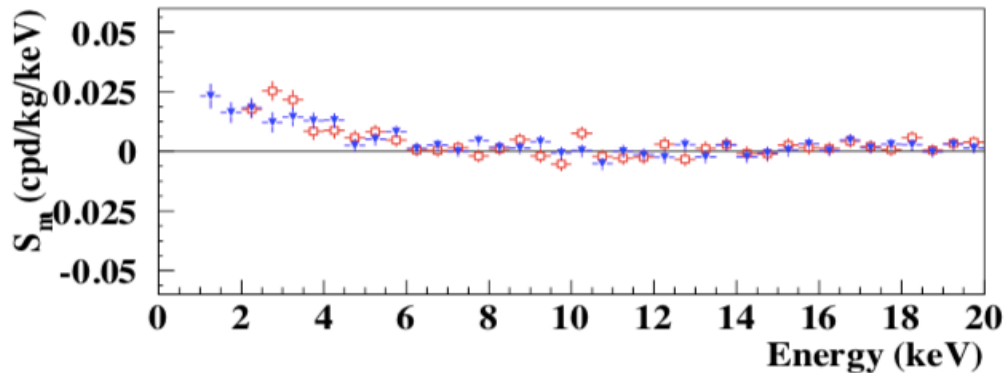
ICHEP2018 SEOUL

DAMA/LIBRA-phase2 in WIMP effective models

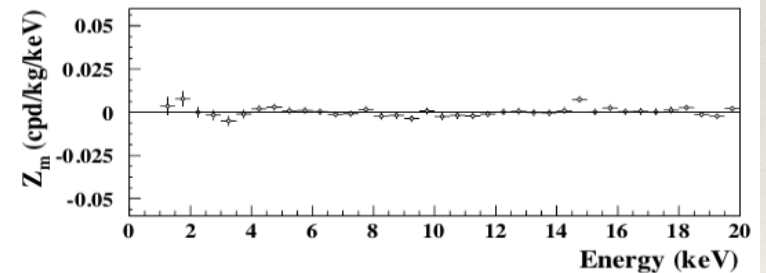
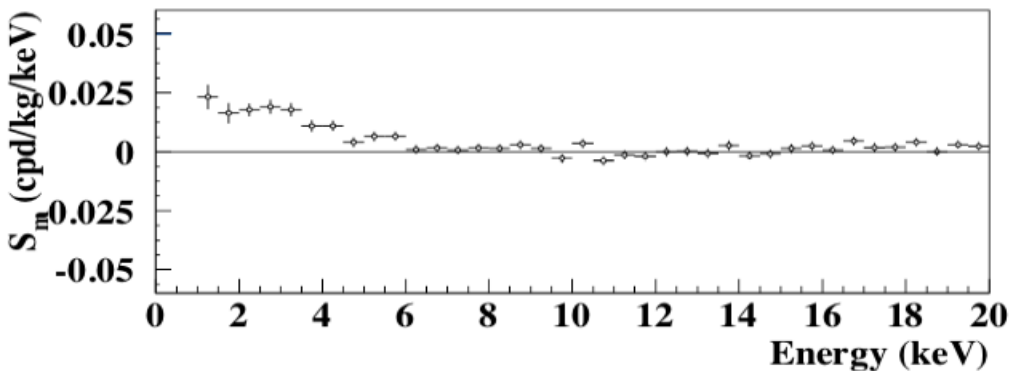
Jong-Hyun Yoon @ Sogang U.
In collaboration with
Prof. Stefano Scopel
Dr. Gaurav Tomar
Mr. Sunghyun Kang

DAMA/LIBRA-phase2 in WIMP effective models

- ❖ DAMA released the first model independent results



Energy	S_m (cpd/kg/keV)	Energy	S_m (cpd/kg/keV)
(1.0–1.5) keV	(0.0232 ± 0.0052)	(6.5–7.0) keV	(0.0016 ± 0.0018)
(1.5–2.0) keV	(0.0164 ± 0.0043)	(7.0–7.5) keV	(0.0007 ± 0.0018)
(2.0–2.5) keV	(0.0178 ± 0.0028)	(7.5–8.0) keV	(0.0016 ± 0.0018)
(2.5–3.0) keV	(0.0190 ± 0.0029)	(8.0–8.5) keV	(0.0014 ± 0.0018)
(3.0–3.5) keV	(0.0178 ± 0.0028)	(8.5–9.0) keV	(0.0029 ± 0.0018)
(3.5–4.0) keV	(0.0109 ± 0.0025)	(9.0–9.5) keV	(0.0014 ± 0.0018)
(4.0–4.5) keV	(0.0110 ± 0.0022)	(9.5–10.0) keV	$-(0.0029 \pm 0.0019)$
(4.5–5.0) keV	(0.0040 ± 0.0020)	(10.0–10.5) keV	(0.0035 ± 0.0019)
(5.0–5.5) keV	(0.0065 ± 0.0020)	(10.5–11.0) keV	$-(0.0038 \pm 0.0019)$
(5.5–6.0) keV	(0.0066 ± 0.0019)	(11.0–11.5) keV	$-(0.0013 \pm 0.0019)$
(6.0–6.5) keV	(0.0009 ± 0.0018)	(11.5–12.0) keV	$-(0.0019 \pm 0.0019)$



$$\begin{aligned}
 S_i(E) &= S_0(E) + S_m(E) \cos \omega(t_i - t_0) + Z_m(E) \sin \omega(t_i - t_0) \\
 &= S_0(E) + Y_m(E) \cos \omega(t_i - t_0).
 \end{aligned}$$

DAMA/LIBRA-phase2 in WIMP effective models

❖ Elastic effective models with the standard Maxwellian

$$\mathcal{H}(\mathbf{r}) = \sum_{\tau=0,1} \sum_{j=1}^{15} c_j^\tau \mathcal{O}_j(\mathbf{r}) t^\tau,$$

$$t^0 = 1, t^1 = \tau_3$$

$$\mathcal{O}_1 = 1_\chi 1_N; \quad \mathcal{O}_2 = (v^\perp)^2; \quad \mathcal{O}_3 = i\vec{S}_N \cdot \left(\frac{\vec{q}}{m_N} \times \vec{v}^\perp\right)$$

$$\mathcal{O}_4 = \vec{S}_\chi \cdot \vec{S}_N; \quad \mathcal{O}_5 = i\vec{S}_\chi \cdot \left(\frac{\vec{q}}{m_N} \times \vec{v}^\perp\right); \quad \mathcal{O}_6 = \left(\vec{S}_\chi \cdot \frac{\vec{q}}{m_N}\right) \left(\vec{S}_N \cdot \frac{\vec{q}}{m_N}\right)$$

$$\mathcal{O}_7 = \vec{S}_N \cdot \vec{v}^\perp; \quad \mathcal{O}_8 = \vec{S}_\chi \cdot \vec{v}^\perp; \quad \mathcal{O}_9 = i\vec{S}_\chi \cdot \left(\vec{S}_N \times \frac{\vec{q}}{m_N}\right)$$

$$\mathcal{O}_{10} = i\vec{S}_N \cdot \frac{\vec{q}}{m_N}; \quad \mathcal{O}_{11} = i\vec{S}_\chi \cdot \frac{\vec{q}}{m_N}; \quad \mathcal{O}_{12} = \vec{S}_\chi \cdot \left(\vec{S}_N \times \vec{v}^\perp\right)$$

$$\mathcal{O}_{13} = i\left(\vec{S}_\chi \cdot \vec{v}^\perp\right) \left(\vec{S}_N \cdot \frac{\vec{q}}{m_N}\right); \quad \mathcal{O}_{14} = i\left(\vec{S}_\chi \cdot \frac{\vec{q}}{m_N}\right) \left(\vec{S}_N \cdot \vec{v}^\perp\right)$$

$$\mathcal{O}_{15} = -\left(\vec{S}_\chi \cdot \frac{\vec{q}}{m_N}\right) \left(\left(\vec{S}_N \times \vec{v}^\perp\right) \cdot \frac{\vec{q}}{m_N}\right),$$

$$\chi^2(m_\chi, \sigma_p, r) = \sum_{k=1}^{14} \frac{\left[S_{m,k} - S_{m,k}^{exp}(m_\chi, \sigma_p, r)\right]^2}{\sigma_k^2}$$

$$(v_T^\perp)^2 = v_T^2 - v_{min}^2.$$

$$v_{min}^2 = \frac{q^2}{4\mu_T^2} = \frac{m_T E_R}{2\mu_T^2},$$

A.L.Fitzpatrick, W.Haxton, E.Katz, N.Lubbers and Y.Xu, JCAP1302, 004

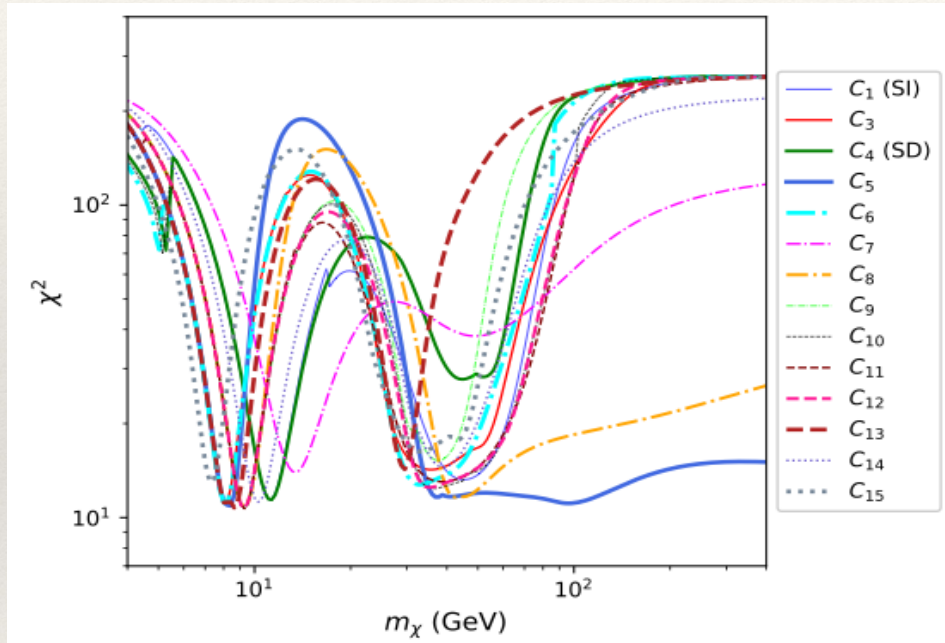
(2013),1203.3542;

N.Anand, A.L.Fitzpatrick and W.C.Haxton, Phys.Rev.C89, 065501

(2014).1308.6288.

DAMA/LIBRA-phase2 in WIMP effective models

❖ Likelihood analysis



$$\chi^2(m_\chi, \sigma_p, r) = \sum_{k=1}^{14} \frac{[S_{m,k} - S_{m,k}^{exp}(m_\chi, \sigma_p, r)]^2}{\sigma_k^2}$$

c_j	$m_{\chi,\min}$ (GeV)	$r_{\chi,\min}$	σ (cm ²)	χ^2_{\min}
c_1	11.17	-0.76	2.67e-38	11.38
	45.19	-0.66	1.60e-39	13.22
c_3	8.10	-3.14	2.27e-31	11.1
	35.68	-1.10	9.27e-35	14.23
c_4	11.22	1.71	2.95e-36	11.38
	44.71	-8.34	5.96e-36	27.7
c_5	8.34	-0.61	1.62e-29	10.83
	96.13	-5.74	3.63e-34	11.11
c_6	8.09	-7.20	5.05e-28	11.11
	32.9	-6.48	5.18e-31	12.74
c_7	13.41	-4.32	4.75e-30	13.94
	49.24	-0.65	1.35e-30	38.09
c_8	9.27	-0.84	8.67e-33	10.82
	42.33	-0.96	1.30e-34	11.6
c_9	9.3	4.36	8.29e-33	10.69
	37.51	-0.94	1.07e-33	15.23
c_{10}	9.29	3.25	4.74e-33	10.69
	36.81	0.09	2.25e-34	12.40
c_{11}	9.27	-0.67	1.15e-34	10.69
	38.51	-0.66	9.17e-37	13.02
c_{12}	9.26	-2.85	3.92e-34	10.69
	35.22	-1.93	2.40e-35	12.47
c_{13}	8.65	-0.26	1.21e-26	10.76
	29.42	0.10	5.88e-29	14.28
c_{14}	10.28	-0.59	2.61e-26	11.21
	38.88	-1.93	2.19e-27	14.48
c_{15}	7.32	-3.58	2.04e-27	12.91
	33.28	4.25	2.05e-33	16.26

Sunghyun Kang, S.S., G. Tomar, J.H. Yoon,

arXiv:1804.07528

DAMA/LIBRA-phase2 in WIMP effective models

❖ Nuclear response functions

coupling	$R_{0k}^{\tau\tau'}$	$R_{1k}^{\tau\tau'}$	coupling	$R_{0k}^{\tau\tau'}$	$R_{1k}^{\tau\tau'}$
1	$M(q^0)$	-	3	$\Phi''(q^4)$	$\Sigma'(q^2)$
4	$\Sigma''(q^0), \Sigma'(q^0)$	-	5	$\Delta(q^4)$	$M(q^2)$
6	$\Sigma''(q^4)$	-	7	-	$\Sigma'(q^0)$
8	$\Delta(q^2)$	$M(q^0)$	9	$\Sigma'(q^2)$	-
10	$\Sigma''(q^2)$	-	11	$M(q^2)$	-
12	$\Phi''(q^2), \tilde{\Phi}'(q^2)$	$\Sigma''(q^0), \Sigma'(q^0)$	13	$\tilde{\Phi}'(q^4)$	$\Sigma''(q^2)$
14	-	$\Sigma'(q^2)$	15	$\Phi''(q^6)$	$\Sigma'(q^4)$

$$R_k^{\tau\tau'} = R_{0k}^{\tau\tau'} + R_{1k}^{\tau\tau'} \frac{(v_T^\perp)^2}{c^2} = R_{0k}^{\tau\tau'} + R_{1k}^{\tau\tau'} \frac{v_T^2 - v_{\min}^2}{c^2}$$

- **M**= vector-charge (scalar, **usual spin-independent part, non-vanishing for all nuclei**)
- **Φ''**=vector-longitudinal, related to spin-orbit coupling $\sigma \cdot l$ (also spin-independent, non-vanishing for all nuclei)
- **Σ'** and **Σ''** = associated to longitudinal and transverse components of nuclear spin, **their sum is the usual spin-dependent interaction, require nuclear spin $j > 0$**
- **Δ**=associated to the orbital angular momentum operator l , also requires $j > 0$
- **Φ'** = related to a vector-longitudinal operator that transforms as a tensor under rotations, requires $j > 1/2$

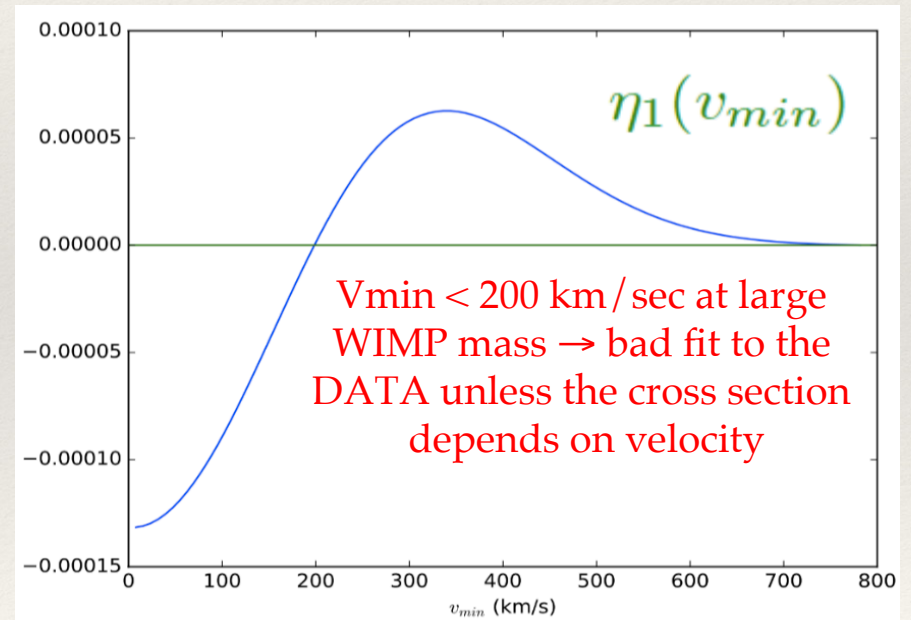
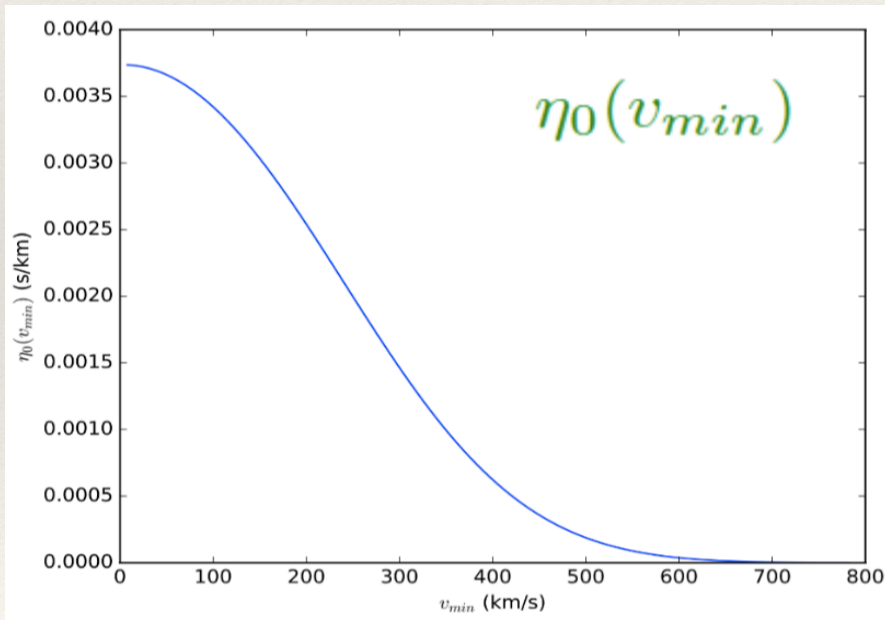
Sunghyun Kang, S.S., G. Tomar, J.H. Yoon,

arXiv:1804.07528

DAMA/LIBRA-phase2 in WIMP effective models

❖ WIMP velocity distribution

$$\eta(v_{min}, t) = \int_{v_{min}}^{\infty} \frac{f(v)}{v} dv = \eta_0(v_{min}) + \eta_1(v_{min}) \cos \omega(t - t_0)$$



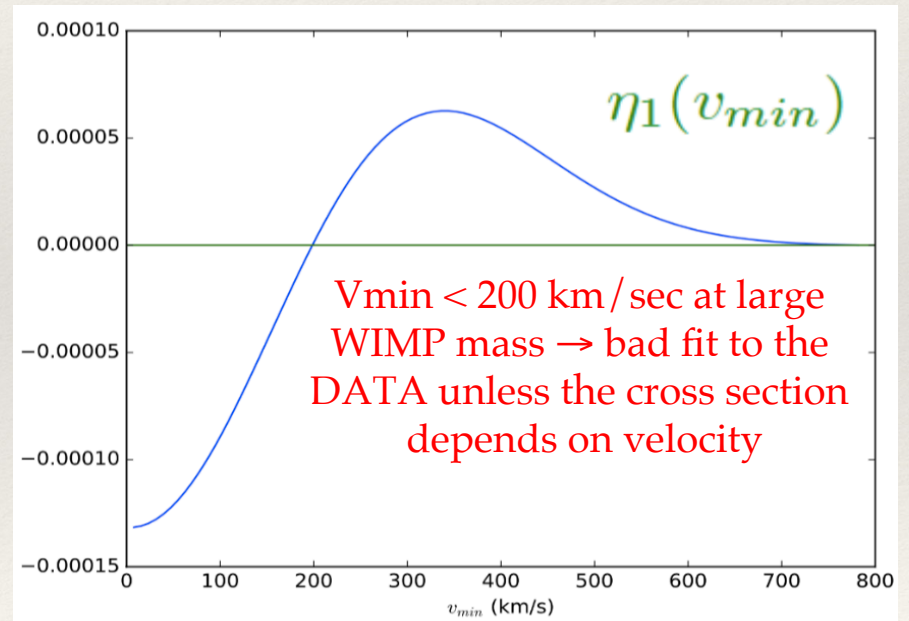
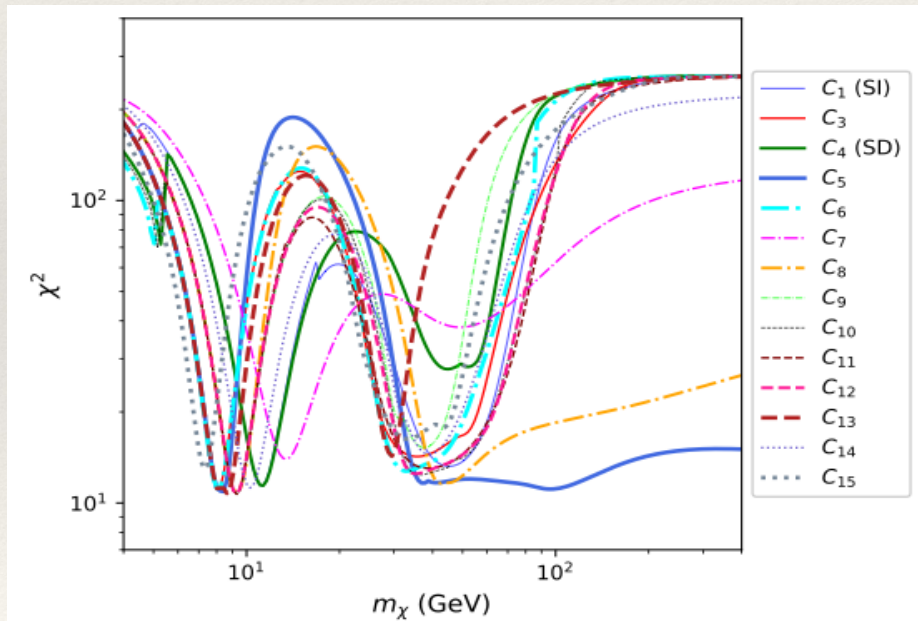
Sunghyun Kang, S.S., G. Tomar, J.H. Yoon,

arXiv:1804.07528

DAMA/LIBRA-phase2 in WIMP effective models

❖ WIMP velocity distribution

$$\eta(v_{min}, t) = \int_{v_{min}}^{\infty} \frac{f(v)}{v} dv = \eta_0(v_{min}) + \eta_1(v_{min}) \cos \omega(t - t_0)$$

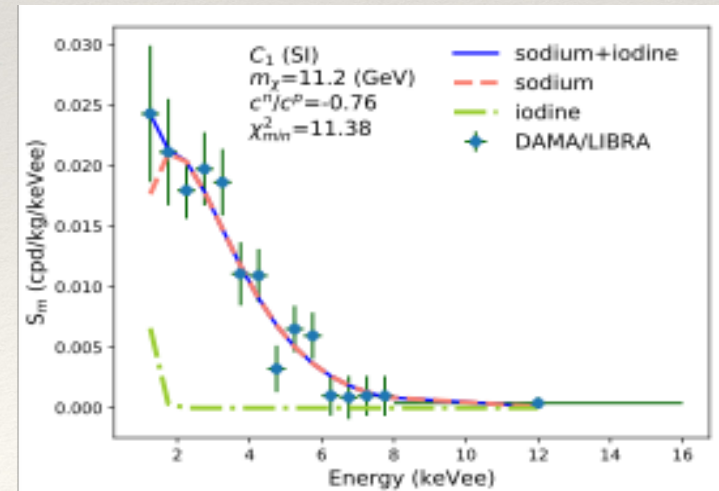
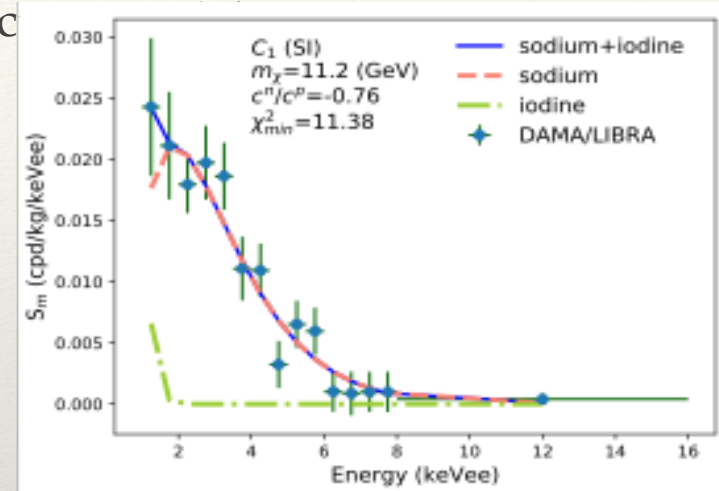
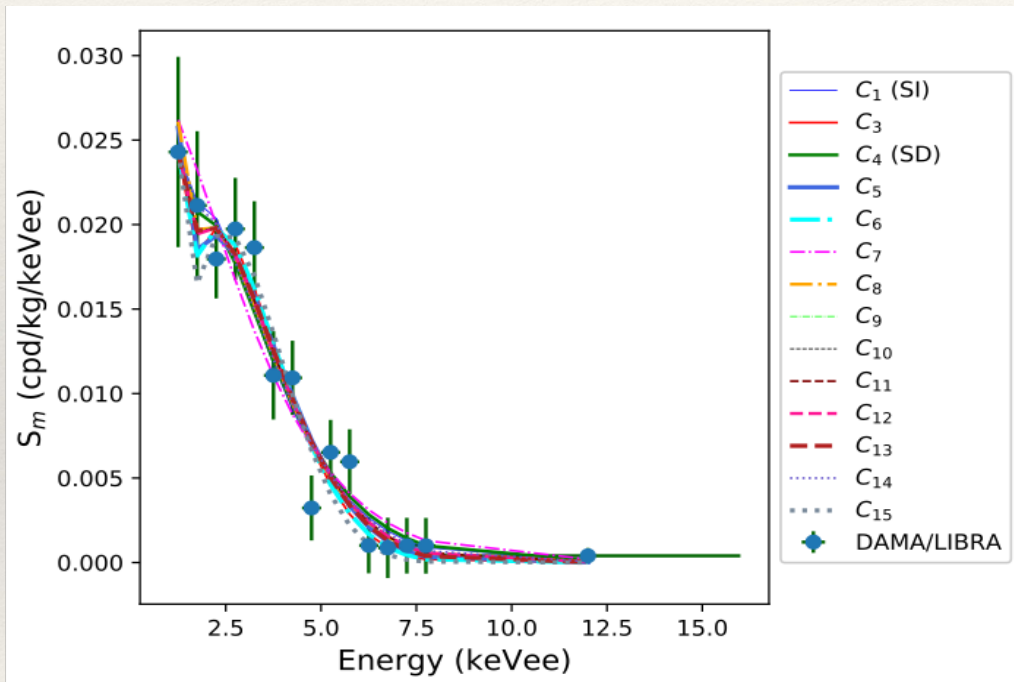


Sunghyun Kang, S.S., G. Tomar, J.H. Yoon,

arXiv:1804.07528

DAMA/LIBRA-phase2 in WIMP effective models

- ❖ DAMA modulation amplitudes as a function of the measured ionization energy E_{ee} for the absolute minima of each effect



$$\sigma_{\chi N} \propto [c^p Z + (A - Z)c^n]^2$$

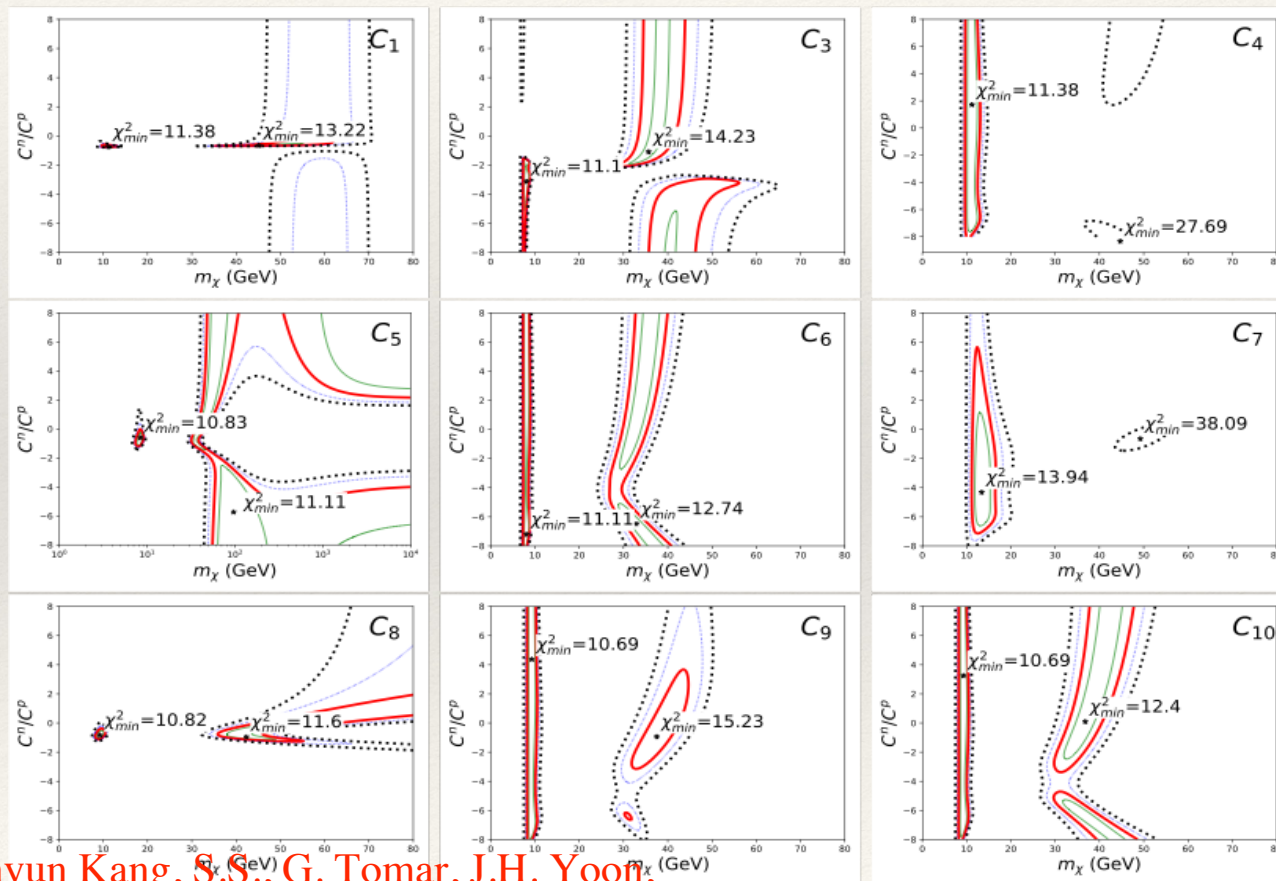
$$r_{Iodine} \simeq -53/(127 - 53) \simeq -0.7 \quad (\simeq -0.9) \text{ for sodium}$$

Sunghyun Kang, S.S., G. Tomar, J.H. Yoon,

arXiv:1804.07528

DAMA/LIBRA-phase2 in WIMP effective models

- Contour plots of χ^2 on the WIMP mass v.s. r plane

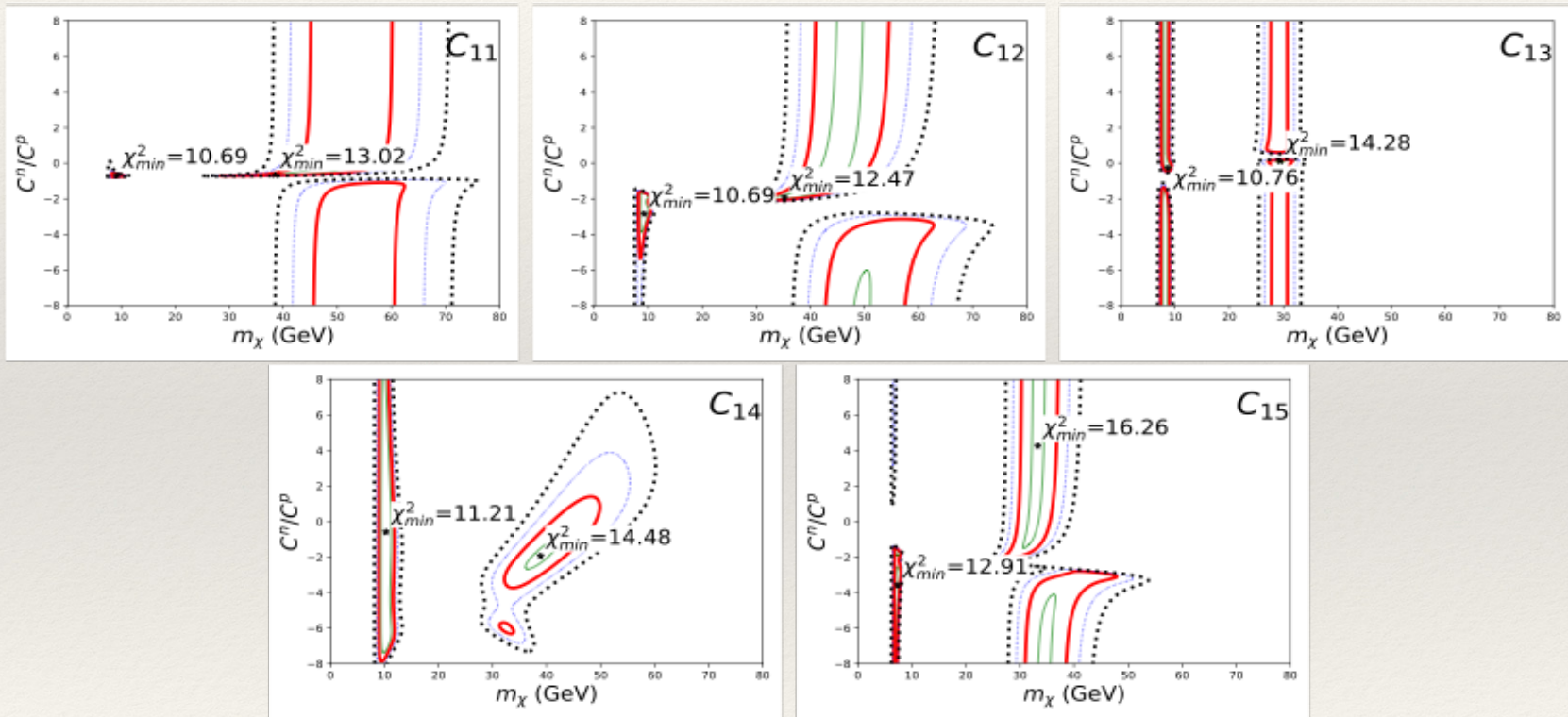


Sunghyun Kang, S.S., G. Tomar, J.H. Yoon,

arXiv:1804.07528

DAMA/LIBRA-phase2 in WIMP effective models

- Contour plots of χ^2 on the WIMP mass v.s. r plane

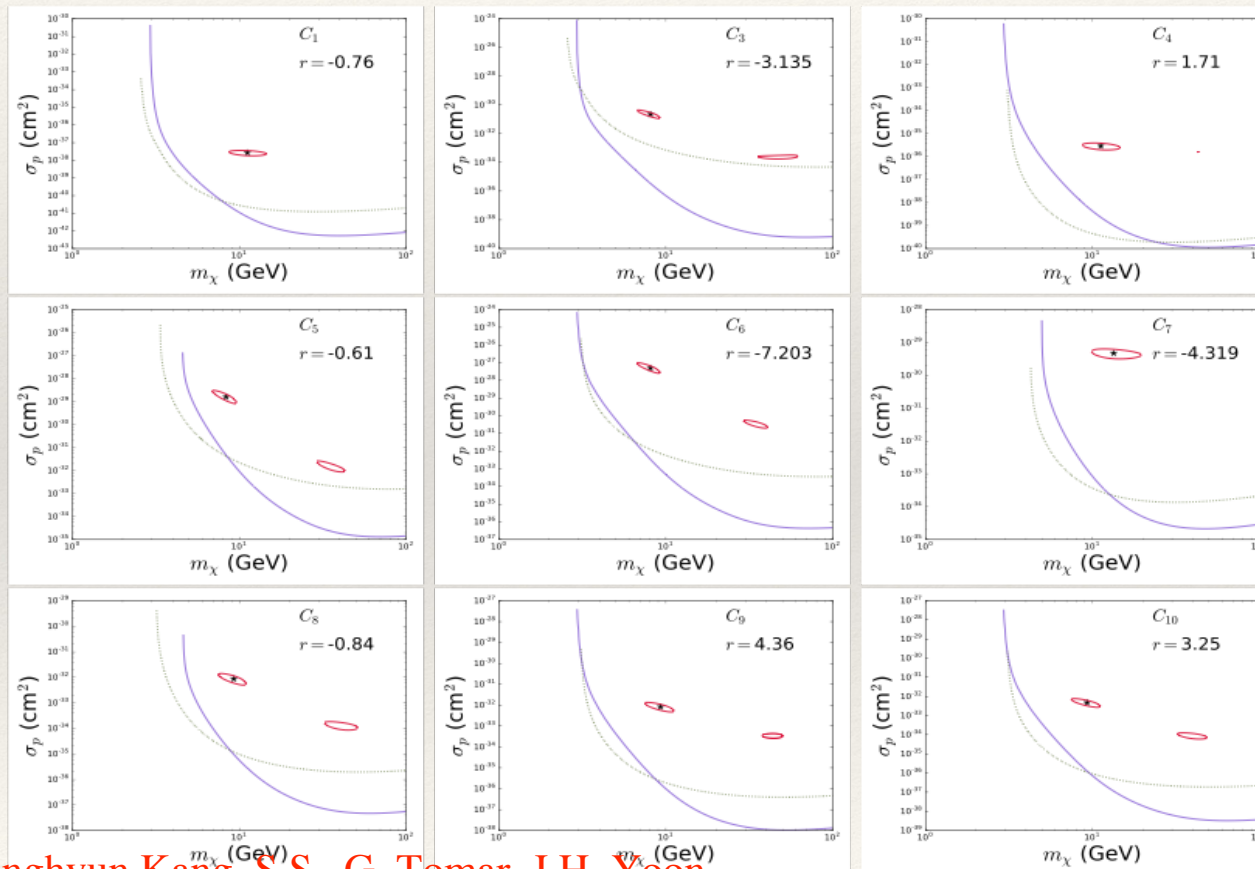


Sunghyun Kang, S.S., G. Tomar, J.H. Yoon,

arXiv:1804.07528

DAMA/LIBRA-phase2 in WIMP effective models

- ❖ 5-sigma best fit DAMA regions with XENON1T(solid purple line) and PICO60(green dots)

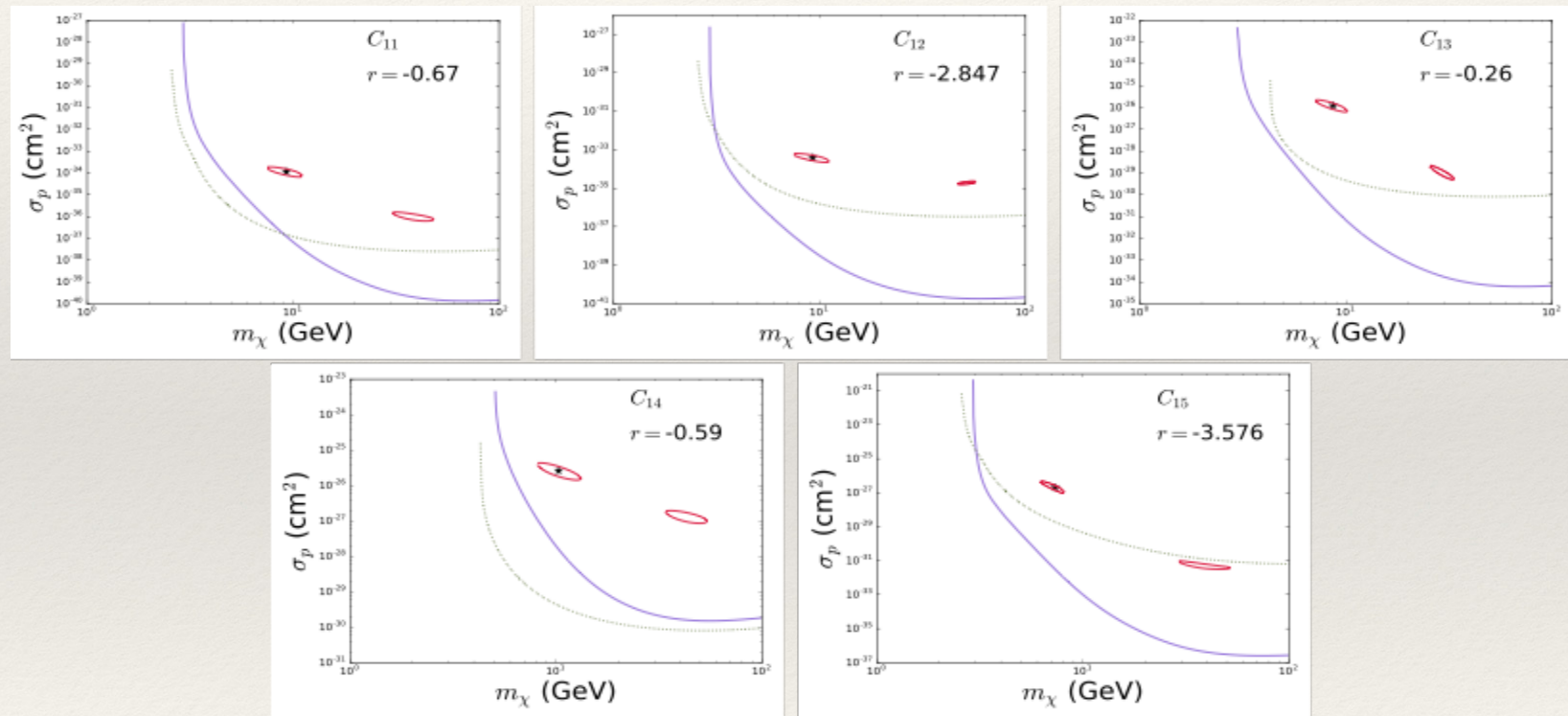


Sunghyun Kang, S.S., G. Tomar, J.H. Yoon,

arXiv:1804.07528

DAMA/LIBRA-phase2 in WIMP effective models

- ❖ 5-sigma best fit DAMA regions with XENON1T(solid purple line) and PICO60(green dots)



Sunghyun Kang, S.S., G. Tomar, J.H. Yoon,

arXiv:1804.07528

Conclusions

- ❖ No fit of the DAMA result is available in the literature in terms of non-relativistic EFT models
- ❖ In addition to increasing the exposure, the phase2 result also includes a lower energy threshold, and the new spectrum of modulation amplitudes no longer shows a maximum, but is rather monotonically decreasing with energy
- ❖ We extended an assessment of the goodness of fit of the new DAMA result to NREFT scenarios
- ❖ All models yield an acceptable χ^2
- ❖ All best-fit minima are inconsistent with the bounds from XENON1T and PICO60

Sunghyun Kang, S.S., G. Tomar, J.H. Yoon,

arXiv:1804.07528